Glueball calculations with the t expansion

C. P. van den Doel and D. Horn
School of Physics and Astronomy, Tel-Aviv University, Tel-Aviv, Israel
(Received 13 November 1986; revised manuscript received 5 January 1987)

We discuss the way glueball states can be calculated using the t-expansion technique for the SU(3) lattice gauge theory in $3+1$ space-time dimensions. Starting with strong-coupling wave functions we specify the simplest glueball structures that can be analyzed. They are described in a general group-theoretical language. We also present an alternative construction in terms of electric and magnetic fields. We then explain the use of the connected matrix formalism for this problem and discuss the results for the 0^{++} and 1^{+-} glueballs that have been analyzed before. We present new results for 0^{--}, 1^{--}, and 2^{--} glueballs, for which we calculated the t expansion to order t^6. They exhibit a scaling behavior leading to masses which are of the order of twice that of the scalar glueball.

I. INTRODUCTION

The t expansion is an analytic method which is suitable for the study of lattice-QCD in the Hamiltonian formulation. It has, so far, been applied to the pure glue sector. In this approximation it is quite useful for estimating masses of glueball states. We report here on the efforts carried out in this direction.

We start in Sec. II by recapitulating the basic elements of the t-expansion technique and the methods that have been developed for its analysis. This is followed in Sec. III by a group-theoretical analysis of the wave functions which we use for the glueball states. These wave functions are the simplest structures which can be created in the strong-coupling description. We describe several possible sets involving two-plaquette structures. A systematic construction of a glueball with any quantum number can be given in terms of color-electric and color-magnetic fields. This method, described in Sec. IV, is more cumbersome but may be unavoidable for some quantum numbers. Section V is devoted to an explanation of the computational techniques that are being used here, in particular the formulation of the t expansion for the mass as an explicit volume-independent series. Section VI contains a presentation and discussion of our old as well as new results. The latter include our analysis of 0^{--}, 1^{--}, and 2^{--} glueballs to order t^6. The last two are degenerate in this order. Using the same techniques employed for the scalar glueball we obtain scaling results which exhibit masses about twice that of the scalar state. The higher angular momenta lie lower than the $J=0$ state. These features follow the strong-coupling pattern in spite of the cumulative effect of hundreds of diagrams which enter into this calculation.

II. THE t EXPANSION FOR SU(3) IN THE STRONG-COUPLING BASIS

The technique of the t expansion was introduced in Ref. 1 and applied to the SU(2) lattice gauge theory in Ref. 2. Its first application to SU(3) was given in Ref. 3. In this chapter we recapitulate the basic elements of the model and the technique used to analyze it.

The theory we study is the $(3+1)$-dimensional SU(3) lattice gauge theory defined by the Kogut-Susskind Hamiltonian[4]

$$H=\frac{g^2}{2}\left[\sum_l \mathbf{E}_l{}^2+x\sum_p (6-\mathrm{tr}U_p-\mathrm{tr}U_p^\dagger)\right], \tag{2.1}$$

where g is the coupling constant and $x\equiv 2/g^4$. The link operators $\mathbf{E}_l$ and U_l which appear in (2.1) are conjugate quantum variables satisfying the commutation relations

$$[E_l^a, U_{l'}]=\frac{\lambda^a}{2}U_l\delta_{ll'}\ . \tag{2.2}$$

Intuitively, the operator E_l^a is the color-electric flux operator associated with the link l, and $\mathrm{tr}U_p$ is the color-magnetic flux operator associated with the plaquette p. The operator U_p is defined to be

$$U_p=U_1U_2U_3{}^{-1}U_4{}^{-1}\ , \tag{2.3}$$

where the product of the unitary link operators U_l is taken in the counterclockwise direction. In carrying out explicit computations it is useful to work with the operator

$$\overline{H}=\sum_l \mathbf{E}_l{}^2-x\sum_p (\mathrm{tr}U_p+\mathrm{tr}U_p^\dagger)\ , \tag{2.4}$$

which is related to (2.1) by an overall multiplicative and additive constant.

In our analysis we employ the t expansion in the same way in which it was applied to the SU(2) theory in Ref. 2. Using the vacuum of the strong-coupling limit $|0\rangle$, which is the state annihilated by the color-electric field

$$\mathbf{E}_l\,|0\rangle=0\ , \tag{2.5}$$

we define the energy function

$$E(t,g^2)=\frac{\langle 0|He^{-t\overline{H}}|0\rangle}{\langle 0|e^{-t\overline{H}}|0\rangle}\ . \tag{2.6}$$

This function tends in the limit $t\to\infty$ to the correct vacu-

um energy. The Taylor series of this function defines the connected matrix elements:

$$E(t)=\frac{g^2}{2}\sum_{n=0}^{\infty}\frac{(-t)^n}{n!}\langle \bar{H}^{n+1}\rangle^c+\frac{6V}{g^2}\ . \tag{2.7}$$

Here V is the total volume (number of plaquettes) of the system. E is an extensive quantity and so are all the connected matrix elements. It was shown in Ref. 1 that the connected matrix elements for any Hamiltonian H and trial wave function $|\psi_0\rangle$ obey the recursion relations

$$\langle H^{n+1}\rangle^c=\langle\psi_0|H^{n+1}|\psi_0\rangle - \sum_{p=0}^{n-1}\binom{n}{p}\langle H^{p+1}\rangle^c\langle\psi_0|H^{n-p}|\psi_0\rangle\ , \tag{2.8}$$

which can be used for their algebraic evaluation.

From the energy function one can extract both the vacuum energy and the 0^{++} glueball mass (first excitation in the vacuum sector). The latter is given by the $t\to\infty$ limit of the expression[2]

$$M(t)\equiv-\frac{g^2}{2}\frac{\partial}{\partial t}\ln\left[-\frac{\partial E(t)}{\partial t}\right]\ . \tag{2.9}$$

The third quantity that we calculate is the string tension. This is obtained by calculating the difference between the ground-state energies of the sector with a string of length L and the sector without any string. The tension $\sigma(t,g^2)$ is defined by dividing this difference by the length L of the string and taking the limit $L\to\infty$. Thus to calculate $\sigma(t,g^2)$ we compute

$$\sigma(t,g^2)=\lim_{L\to\infty}\frac{1}{L}\left[\frac{\langle 0|S^\dagger He^{-t\bar{H}}S|0\rangle}{\langle 0|S^\dagger e^{-t\bar{H}}S|0\rangle}-E(t,g^2)\right]\ , \tag{2.10}$$

where the operator S creates a straight infinite string along one axis; i.e.,

$$S=\prod_{l=(-L/2,0,0)}^{(L/2,0,0)}U_l\ . \tag{2.11}$$

All these quantities refer of course to values of operators defined for lattice QCD. To extract physical information we have to study quantities which are expected to scale in the continuum limit. Such a quantity is the ratio

$$R\equiv\frac{M(t)^2}{\sigma(t)}\ . \tag{2.12}$$

Having obtained an algebraic series for both $\sigma(t)$ and $M(t)$ we are in a position to construct one also for R. This was used successfully both for the SU(2) theory[2] and the SU(3) one.[3]

To calculate masses of other glueballs one has to construct states with different quantum numbers. One such example is the axial glueball which was studied in Ref. 5. The general method consists of constructing appropriate wave functions in the extreme strong-coupling limit and operating on them with the t-expansion technique. The structure of these states is studied in the next section.

III. GLUEBALL WAVE FUNCTIONS

In the strong-coupling limit the vacuum $|0\rangle$ is defined as the state annihilated by all electric field operators. The gauge-invariant excitations are given by acting on $|0\rangle$ with the magnetic operator $\mathrm{tr}\,U_p$. We require the wave functions to be translationally invariant, i.e., represent zero-momentum states. We also like to classify them according to the octahedral group, the cubic symmetry group, in order to be able to read off their corresponding quantum numbers in the continuum. Therefore, let us start with a short description of the octahedral group following the paper by Johnson.[6]

The octahedral group consists of 24 elements which map the cube onto itself. These operations may be interpreted as permutations of the four main diagonals of the cube; therefore, it is isomorphic to S_4. There are five conjugacy classes in this group; hence, there exist five different irreducible representations. Table I is the character table for this group. The notation C_n refers to rotations of the cube by angles of $2\pi/n$. The classes C_2 and C_4 refer to rotations about the coordinate axes, C_3 includes rotations about the main diagonals, and C_2' are rotations about axes parallel to the face diagonals.

The classification of the single-plaquette wave functions was already given by Kogut, Sinclair, and Susskind.[7] Let us derive their results by using the group-theoretical analysis. We start by noting that there are six different wave functions at our disposal. Three of them are given by using one of the three loops in Fig. 1, each representing an operation by $\mathrm{tr}\,U_p$, and constructing a translationally invariant superposition from it. We will designate these states $|1\rangle$, $|2\rangle$, and $|3\rangle$ accordingly. The three other states are constructed similarly by using $\mathrm{tr}\,U_p^\dagger$. They can be represented by arrows drawn in the opposite direction and designated by $|-1\rangle$, $|-2\rangle$, and $|-3\rangle$. Clearly we will not get all possible representations of the octahedral group this way, because we have just six states. It is easy to verify that we obtain the representations A_1, T_1, and

TABLE I. Character table for the octahedral group.

Representation \ Multiplicity / Class	1 I	3 C_2	8 C_3	6 C_4	6 C_2'	Lowest J
A_1	1	1	1	1	1	0
A_2	1	1	1	−1	−1	3
E	2	2	−1	0	0	2
T_1	3	−1	0	1	−1	1
T_2	3	−1	0	−1	1	2

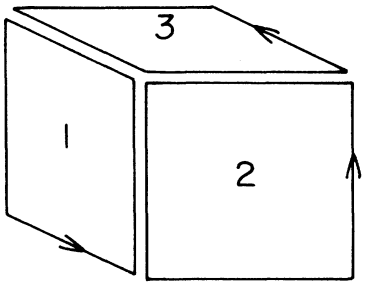

FIG. 1. Graphic notation for the operation of $\mathrm{tr}\, U_p$ on three different faces of a cube.

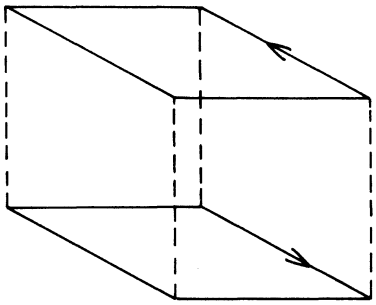

FIG. 2. A state created by simultaneous operation of $\mathrm{tr}\, U_p$ and $\mathrm{tr}\, U_p^\dagger$ on the vacuum $|0\rangle$. The two different plaquettes are located on opposing faces of one cube.

E. The representation A_1 is just the scalar state:

$$|S\rangle = |1\rangle + |-1\rangle + |2\rangle + |-2\rangle + |3\rangle + |-3\rangle \ . \quad (3.1)$$

The representation T_1 is three dimensional. The basis is defined by combinations such as

$$|A_x\rangle = |1\rangle - |-1\rangle \ . \quad (3.2)$$

Finally, the representation E has two components given by

$$|1\rangle + |-1\rangle - |2\rangle - |-2\rangle$$

and

$$|1\rangle + |-1\rangle + |2\rangle + |-2\rangle - 2|3\rangle - 2|-3\rangle \ .$$

By comparing with the characters of the rotation group one finds that the state $|S\rangle$ of the representation A_1 is a scalar, the states of the representation T_1 are the three components of angular momentum $J=1$, while the two states of E are appropriate projections of $J=2$.

The parity of a state is determined by the behavior of its wave function under lattice inversion, and its charge conjugation by its transformation property under arrow inversions. All our six original states are even under parity; hence, the quantum numbers J^{PC} of the one-plaquette glueball states are found to be 0^{++}, 1^{+-}, and 2^{++}.

If we wish to obtain other quantum numbers we have to invoke more complicated structures. In the rest of this section we will discuss several such structures which are constructed by the simultaneous operation with two plaquettes. An example of this kind is given in Fig. 2. Here we have two plaquettes on two opposing faces of a cube: one representing the operation of $\mathrm{tr}\, U_p$ and the other that of $\mathrm{tr}\, U_p^\dagger$ on the vacuum state $|0\rangle$. By taking a translationally invariant superposition of this structure we form the state $|3,-3\rangle$ employing a notation which is an obvious generalization of the one used above for the single-plaquette states. Once again we find that there are six different states that we can form this way. But, whereas the one-plaquette states were invariant under space inversion, we find that these two-plaquette states transform into one another; thus,

$$P|3,-3\rangle = |-3,3\rangle \ . \quad (3.3)$$

It is then obvious that by taking linear superpositions

$$|3,+\rangle = |3,-3\rangle + |-3,3\rangle$$

and

$$|3,-\rangle = |3,-3\rangle - |-3,3\rangle \ ,$$

we obtain states which have $P=C=+$ and $P=C=-$, respectively. We are left therefore with only three states of each kind to form bases for irreducible representations of the octahedral group. By taking a symmetric combination of all directions one forms the A_1 representations, corresponding to quantum numbers of 0^{++} and 0^{--}. The remaining states can be used to form E representations, fitting the quantum numbers of 2^{++} and 2^{--}. We will be particularly interested in the 0^{--} state because it has exotic quantum numbers and is so easily described in this formalism.

Next let us look at structures of the type depicted in Fig. 3 which we will refer to as "window" diagrams.

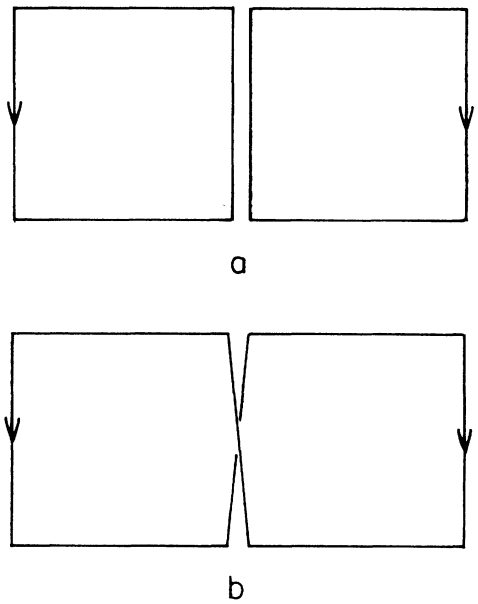

FIG. 3. Window diagrams. (a) A state generated by the operation of $\mathrm{tr}\, U_p$ and $\mathrm{tr}\, U_p^\dagger$ on two neighboring plaquettes. (b) A state of similar character generated by a loop of length eight. The linear combination of type a-b corresponds to a $\bar{3}$ representation on the common link.

These are two-plaquette states in which the two plaquettes are nearest neighbors on the same plane with the arrows on the joint link pointing in the same direction. Let us denote the corresponding states by $|ab\rangle$ if the two-plaquette structure lies in the ab plane and the direction of the common link is a. If the common link points in the opposite direction we will denote the state by $|-ab\rangle$. Clearly these two states are charge conjugates of one another. Since they can also be related to one another by reflection all our irreducible representation will have $P=C$. We can form bases of the representations by considering combinations of the type

$$|x,cd\rangle = |xy\rangle + c\,|xz\rangle + d\,|-xy\rangle + cd\,|-xz\rangle\ , \qquad (3.4)$$

where the parameters c and d take the values 1 or -1. All 12 states can be described in this way by adding all obvious permutations where y or z are the common axes. The value of d is equal to that of P and C.

For the combination $c=d=1$ we obtain the A_1 and E representations with the corresponding 0^{++} and 2^{++} lowest states. The scalar state is given by the symmetric superposition

$$|x,++\rangle + |y,++\rangle + |z,++\rangle$$

in complete analogy with the scalar combination of the single-plaquette states, Eq. (3.1). The basis for the irreducible representation E can also be constructed in the same way as in the single-plaquette case. Using $c=-d=1$ we find a basis for the representation T_1 whose lowest state corresponds to 1^{--}. $c=-d=-1$ leads to a mixture of the irreducible representations A_2 and E, whose lowest states will be 3^{++} and 2^{++}, respectively. The representation A_2 is given by the symmetric combination

$$|x,-+\rangle + |y,-+\rangle + |z,-+\rangle$$

and E is again constructed by the two remaining orthogonal states. Finally, for $c=d=-1$ we obtain the T_2 representation corresponding to a 2^{--} state. It should be noted that the same kind of classification holds separately for the structures depicted in Figs. 3(a) and 3(b). A sum or difference of the two corresponds to the choice of a **6** or $\bar{\mathbf{3}}$ representation on the joint link. To obtain the lowest state in the strong-coupling limit one should choose of course the difference.

In Sec. VI we report calculations carried out for states with $d=-1$. These are states which include in every plane a structure with negative charge conjugation. This structure cannot be removed by operating twice with the Hamiltonian; hence, the number of diagrams that have to be calculated for these states is much smaller than for positive charge conjugation. Thus we will obtain results for 1^{--} and 2^{--} states. Since, to the order t^6 to which we carry out our calculations there is no significant connected matrix element between two perpendicular planes, the sign of c is irrelevant. Hence both these states, which correspond to the irreducible representations T_1 and T_2, have identical mass functions.

Finally let us study the family of "wing" diagrams shown in Fig. 4. All these diagrams can be described by two neighboring plaquettes on a cube. Using the notation of Fig. 1 we can classify all 24 possible diagrams by specifying the two plaquettes as well as the direction of the magnetic flux (in or out of the cube). Parity is defined by reflection through the center of the cube and charge conjugation by arrow reversal. This leads to relations of the following kind:

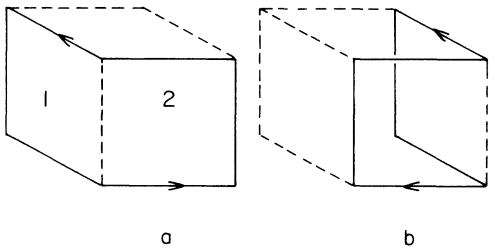

FIG. 4. Wing diagrams. States generated by loops of length six which wrap around two neighboring faces of a cube. Using the notation explained in the text they represent the states (a) $|1,2,\text{out}\rangle$, (b) $|1,-2,\text{in}\rangle$.

$$|1,2,\text{out}\rangle \leftarrow PC \rightarrow |-1,-2,\text{out}\rangle\ ,$$

$$|1,-2,\text{out}\rangle \leftarrow PC \rightarrow |-1,2,\text{out}\rangle\ ,$$

$$|1,2,\text{out}\rangle \leftarrow C \rightarrow |-1,-2,\text{in}\rangle\ ,$$

$$|1,-2,\text{out}\rangle \leftarrow C \rightarrow |-1,2,\text{in}\rangle\ .$$

Since operations of the cubic octahedral group do not change an out state into an in state we can analyze the two families separately. Their linear superpositions will give the two possible values of C with the same value of PC.

We define the combinations

$$|z,cd,\text{out}\rangle = |1,2,\text{out}\rangle + c\,|-1,-2,\text{out}\rangle + d\,|1,-2,\text{out}\rangle + cd\,|-1,2,\text{out}\rangle \qquad (3.5)$$

and similarly for the in states and all permutations of the axes. Again c and d take the values of 1 and -1. The value of c specifies the sign of the product PC. Out of these combinations we form bases for the irreducible representations. The A_1 representation is obtained from the symmetric combination

$$|x,++,\text{out}\rangle + |y,++,\text{out}\rangle + |z,++,\text{out}\rangle$$

and similarly for the in states. The sum and difference of these two form yet another description of the quantum numbers 0^{++} and 0^{--}. The E representation is obtained from the two orthogonal combinations of $c=d=1$ leading to 2^{++} and 2^{--} wave functions. The three states with $c=-d=1$ form bases for the irreducible representation T_2, corresponding to alternative wave functions for 2^{++} and 2^{--}. The negative PC states form groups of three-dimensional representations. The three vectors are given by

$$|z,-+\rangle + e\,|y,--\rangle,\quad |y,-+\rangle + e\,|x,--\rangle\ ,$$

$$|x,-+\rangle + e\,|z,--\rangle\ .$$

For $e=1$ they form a T_1 representation, describing wave

functions for 1^{+-} and 1^{-+} states. $e=-1$ leads to a basis for the T_2 representation corresponding to the quantum numbers 2^{+-} and 2^{-+}. We have not yet carried out calculations for these states. We present this analysis of the wing diagrams in order to point out the richness of the spectrum that can be calculated from two-plaquette wave functions. We learn also that the same quantum numbers can appear in different wave functions. This should allow us in the future to carry out several calculations which can serve as a check on each other.

IV. GLUONIC OPERATORS AND GLUEBALL FIELDS

A systematic search for glueball operators was carried out in Ref. 8 for the 4-dimensional Euclidean formulation of lattice QCD. Using the group-theoretical structure of the hypercubical symmetry, Mandula *et al.* classified all possible operators that can be obtained from products of the color-magnetic and -electric fields. The magnetic color field can be defined by

$$B^a=\frac{1}{8i}\sum \mathrm{tr}\left[\frac{\lambda^a}{2}U_p-\mathrm{H.c.}\right], \tag{4.1}$$

where the sum goes over the four plaquettes which are orthogonal to the same axis and share one vertex, as depicted in Fig. 5. U_p is the product of the unitary link operators U_l taken in the counterclockwise direction as in Eq. (2.3). The arrows on the plaquettes in Fig. 5 indicate the direction which enters the sum with a positive sign. The term $\lambda^a/2$ should always appear in the appropriate location of the common vertex. Obviously a structure such as this is reproduced through reflection in the common vertex, while it obtains a negative sign under arrow reversal. Therefore it has the correct characteristics for a 1^{+-} operator associated with the given vertex and direction, and it is an octet under the color gauge group at this vertex.

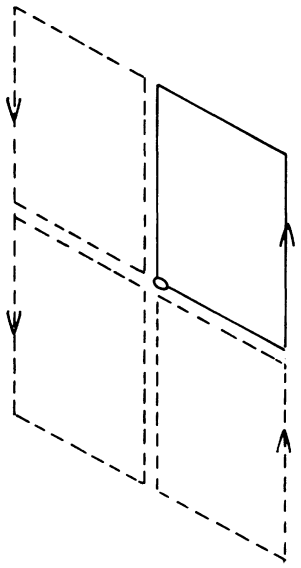

FIG. 5. The definition of the B field involves the sum of terms defined in Eq. (4.1) over four plaquettes as shown here.

The electric field operator is also associated with a vertex and a direction on the lattice. Its operation on a link field which lies in the positive direction is defined in Eq. (2.2). By taking various tensor products of the electric and magnetic fields one can build up in a systematic way glueball fields with all quantum numbers. The simplest example is the pseudoscalar given by the scalar product of these two operators: $\sum_{a,i}E_i^aB_i^a$. However, when applied to the strong-coupling vacuum this operator will annihilate it, since every electric field component annihilates $|0\rangle$. Hence, to obtain an appropriate pseudoscalar state we should first create a scalar one, e.g., $H|0\rangle$, and then apply to it $\sum_{a,i}E_i^aB_i^a$. The result of applying E^a to this state is given by

$$E^aH|0\rangle\sim\sum \mathrm{tr}\left[\frac{\lambda^a}{2}U_p-\mathrm{H.c.}\right]|0\rangle\ , \tag{4.2}$$

where the sum extends over the eight plaquettes which share a given direction and a common vertex, as depicted in Fig. 6. Once again we insert arrows to denote the loops which enter the sum with a positive sign. Note that this structure is odd under both reflection through the common vertex and under arrow reversal. Hence it is the appropriate structure for the 1^{--} color state. By applying B^a to this expression and combining the structures of Figs. 5 and 6, we obtain 32 combinations of two-plaquette products which enter into the definition of the basic unit in the pseudoscalar wave function. The contraction of the color indices follows the basic rule

$$\sum_a(\lambda^a)_{ij}(\lambda^a)_{km}=2\delta_{im}\delta_{jk}-\tfrac{2}{3}\delta_{ij}\delta_{km} \tag{4.3}$$

which implies that we can rewrite it as a sum of configurations of closed loops. In addition to this contraction we have to sum over the three space directions and all translations to construct the appropriate 0^{-+} state with zero momentum.

We have given this explicit construction as a key to the general definition of any glueball wave function. It should however be clear from the discussion in Sec. III that it is not necessary to go through this construction to form a candidate for a wave function. In particular, it may suffice to use one component of a given construction in terms of electric and magnetic fields to obtain the ap-

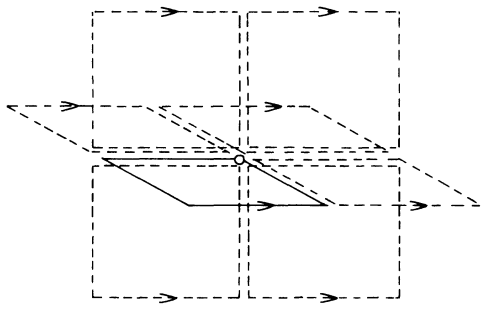

FIG. 6. Operating with E on the scalar state $H|0\rangle$ results in the sum of terms given in Eq. (4.2) over eight plaquettes which share a common vertex and direction as shown here.

propriate quantum numbers of a state that one looks for. An appropriate example is again the pseudoscalar state. The last term of Eq. (4.3) tells us that we can construct a 0^{-+} state with pairs of two closed plaquettes (i.e., pairs of $\mathrm{tr}\,U_p$ operators) as long as they are taken in the particular combination and phases implied by the combination of Figs. 5 and 6.

V. COMPUTATIONAL TECHNIQUES

The calculation of the 0^{++} glueball is different from all the other ones. The reason is that the scalar state belongs to the same quantum-mechanical sector as the vacuum. Therefore it is necessary to ensure that the state of the glueball excitation is orthogonal to the one that we use to contract onto the vacuum. Rather than using the state $|S\rangle$ of Eq. (3.1) we employ a Gram-Schmid procedure in which the Hamiltonian is used to generate the excitations. This results in Eq. (2.9). For particles which have quantum numbers different from the vacuum, we use the strong-coupling state as a new $|\psi_0\rangle$ in our calculation and subtract from its energy the vacuum energy to obtain a prediction for the mass.

We have been careful to choose particle states that carry zero momentum. Their wave functions are therefore spread all over the infinite lattice. One can use the translational invariance of these states to bring the calculation into a format in which the t expansion for the mass of any particular excitation is an explicit volume-independent expression. This was explained in Ref. 5 where the calculation for the axial glueball was carried out. It can be generalized for any other state. The principal idea is to start from some geometric unit on the lattice which carries all the symmetry ingredients of the state. Representing the wave function as a sum over such units on the lattice

$$|\phi\rangle=\frac{1}{N^{1/2}}\sum_i |\phi_i\rangle \tag{5.1}$$

we may utilize translation invariance and single out the geometric unit near the origin ($i=0$) to express any moment of the Hamiltonian in an asymmetric fashion:

$$\langle\phi|H^n|\phi\rangle=\sum_i \langle\phi_i|H^n|\phi_0\rangle\ . \tag{5.2}$$

The basic geometric unit for single-plaquette wave functions is a cube. This is further simplified for the axial state of Eq. (3.2) because only a single plaquette is involved in every cube. The two-plaquette states of Fig. 2 still have a single cube as the basic geometric structure. This is also true for the wing diagrams of Fig. 4; however, the window diagrams of Fig. 3 need a cross built out of four plaquettes to accommodate on it the structure of Eq. (3.4).

The connected-matrix formulation can be applied to expressions of the form of Eq. (5.2). Thus we may define

$$\langle H^{n+1}\rangle_\phi^c=\sum_i \langle\phi_i|H^{n+1}|\phi_0\rangle - \sum_{p=0}^{n-1}\binom{n}{p}\langle H^{p+1}\rangle_\phi^c\sum_i\langle\phi_i|H^{n-p}|\phi_0\rangle\ , \tag{5.3}$$

which serves the same purpose as (2.8) for the vacuum. In fact, subtracting from Eq. (5.3) the vacuum-connected matrix elements, one obtains the coefficients for the t expansion of the mass of the particle represented by the state $|\phi\rangle$. All the relevant diagrams for these coefficients involve geometric forms which are attached to the special unit at $i=0$.

Once the diagrams are calculated we are faced with the choice of what functions to analyze and how to carry out the analysis. Since we are looking for functions which should include information relevant for QCD in the continuum, we investigate ratios of physical quantities of the same dimension. Our hope is that the t expansion is carried out to an order which is large enough to exhibit the scaling behavior which should set in for such ratios in the weak-coupling regime. The ratios that we look at are either R of Eq. (2.12) or the ratios of two masses. Each such expression is given by a power series in t which we have to fit with some Padé procedure. Our standard method is the D-Padé one[1] wherein we perform a nondiagonal Padé analysis of the t derivative of the power series and then integrate it out to $t=\infty$. There is no Padé fit carried out over the y dependence of our expressions. However, we allow ourselves the liberty to perform the D-Padé analysis on the y derivative of the function and afterwards to integrate the approximant over y. Clearly, if the series is long enough, this y procedure should not give an answer different from the application of D-Padé to the original series. However, in practice, the answers may be different. If such difference occurs, we use the version which seems closest to scaling, i.e., the one which develops a plateau beyond the crossover from strong to weak coupling.

VI. DISCUSSION OF RESULTS

The analysis of the vacuum energy density to order t^9 and the scalar glueball mass to order t^7 was carried out in Ref. 3 and that of the axial glueball to order t^7 in Ref. 5. From the specific heat behavior we know that the crossover from strong to weak coupling occurs around $y=2/g^2\approx 1.6$. In the region of $y>1.6$ we look, therefore, for scaling results.

We have redone the analysis for the 0^{++} and 1^{+-} states and corrected some errors which we have discovered in the old calculation. The qualitative results remain the same as in Refs. 3 and 5. The ratio R for the 0^{++} state has several D-Padé approximants which tend to a constant value around $y\approx 2$, these are shown in Fig. 7. They point at a value of $R\approx 9$ in the region of $y\approx 2$. Using $\sqrt{\sigma}=420$ MeV this leads to the estimate of $M=1.3$ GeV. For the 1^{+-} we find that all D-Padé approximants lead to consistent results however they do not seem to scale. The averages of the approximants which are based on the t series of orders 5, 6, and 7 all show an increase beyond $y=1.5$. This is displayed in Fig. 8. It is interesting to note that we find here that the 3-3 diagonal Padé has the same behavior as the other curves below $y=1.5$ but it drops towards zero beyond this point. There are two possible interpretations of this behavior. One is that the true R curve should indeed increase and reach its scal-

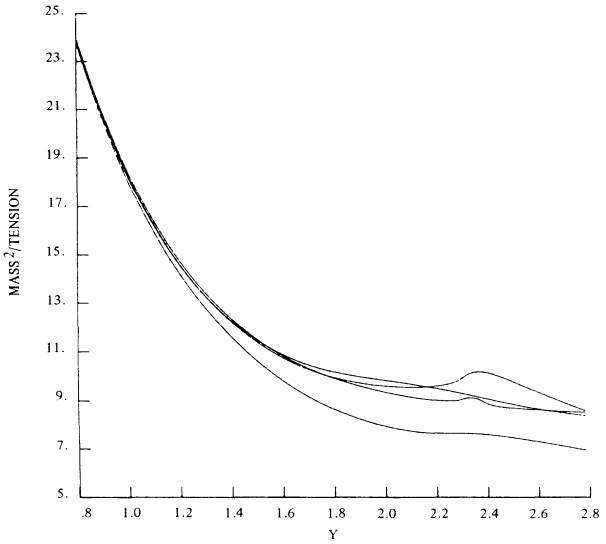

FIG. 7. The D-Padé approximants for the ratio M^2/σ of the scalar glueball which lead to scaling results are displayed vs $y=2/g^2$. The highest curve is the 1-4 and the lowest is the 1-3 D-Padé approximant. The second from bottom is the average of the 1-5 and 2-4 D-Padé (both represent information from a t^7 series) and the second from top is the diagonal 2-2 Padé evaluated at asymptotic t.

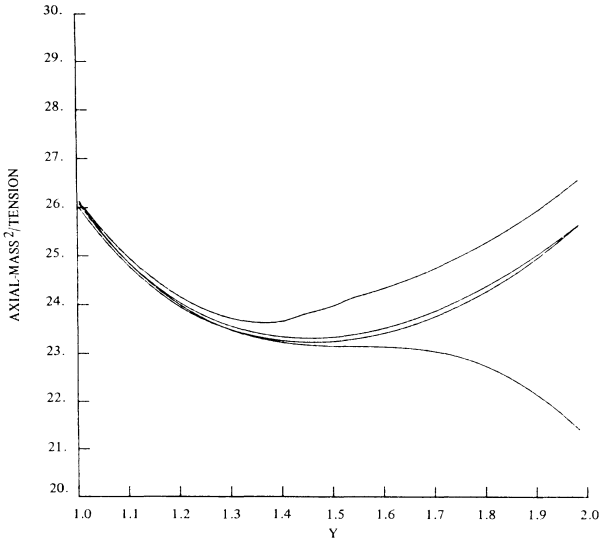

FIG. 8. The $R=M^2/\sigma$ curves for the 1^{+-} state show a different behavior from the scalar ones. The highest curve is the average of all D-Padé approximants of the t^5 series, and the next two represent the averages of the t^6 and t^7 D-Padé approximants. The lowest curve is the 3-3 diagonal Padé of the t^6 series evaluated at asymptotic t.

ing value for higher y. The second is that the scaling behavior will set in only for much higher series but we may use the extremum of $R\approx 23$ observed in Fig. 8 as an educated guess of the final asymptotic value. This would lead to a mass which is 1.6 times heavier than the scalar one, in agreement with the conclusion of Kogut, Sinclair, and Susskind[7] which was based on a Padé analysis of the strong-coupling series.

The axial glueball calculation was the simplest that could be carried out for the single-plaquette states because it involved only a single plaquette per cube. This is also intimately connected to the fact that it is an odd charge-conjugation state. Similarly we find that for two-plaquette states the combinations corresponding to odd charge conjugation involve the smallest number of diagrams that have to be calculated. Nonetheless we end up evaluating more than 200 connected matrix elements in our analysis of 0^{--} and 1^{--} states to order t^6. We generate the first state by diagrams of the type of Fig. 2, and the second from the window diagrams of Fig. 3. Operating on the odd charge-conjugation combinations corresponding to Fig. 3 we find that to this order of the calculation we have only two nonvanishing diagrams which connect two perpendicular planes. Hence our results cannot distinguish between the two possible values of c in Eq. (3.4), and the series of the 1^{--} state of representation T_1 is practically degenerate with the one for the 2^{--} state of T_2.

In the new cases which we present here we find that all D-Padé approximants give consistent results. The curves in Fig. 9 represent their averages for the 0^{--} and 1^{--} glueballs. In both cases we show also the 3-3 diagonal Padé which coincides with the other curves in the neighborhood of $y\approx 2$. These curves have much higher values than those of the scalar glueball in Fig. 7 but they have very similar trends. The ratio of the average of the curves in Fig. 8 to that of Fig. 7 is a slowly varying function. Using the square root of this ratio we obtain numbers for the ratio of $M_{0^{--}}/M_{0^{++}}$ and $M_{1^{--}}/M_{0^{++}}$. These ratios start out as 2 and 1.75, respectively, at $y=0$ for the type of wave functions which we have used. At $y=2$ we find them to be about 2.2 and 1.9, respectively. It is interesting to contrast this small deviation with the different behavior of the axial state. The R curves of the 1^{+-} displayed a characteristically different behavior from those of the 0^{++}. The effect of the high-order diagrams in the 1^{+-} led to completely different characteristics of these curves and to an increasing ratio of $M_{1^{+-}}/M_{0^{++}}$ (which started out as 1 for $y=0$). In the 0^{--} and 1^{--} cases the high-order diagrams lead to a stabilization of the R curves. Nonetheless, the scale of these curves is strongly influenced by the leading y^{-1} behavior, i.e., the strong-coupling ratios prevail.

The glueball states are, of course, only part of the hadronic spectrum of the flavor-singlet mesons. The other part is given by bound states of quarks and antiquarks. In reality the two different kinds can mix in channels with identical quantum numbers, but the total number of states will remain invariant. The interference between the different kinds of structures with the same quantum numbers may also lead to observable effects. This argument was the origin of an early suggestion for searches of vector glueball states[9] in the mass region above the open-charm threshold in e^+e^- annihilation.

It is interesting to note that our prediction for the vector mass is quite high, of the order of 2.5 GeV. Both new states which were calculated here lie near the edge of the

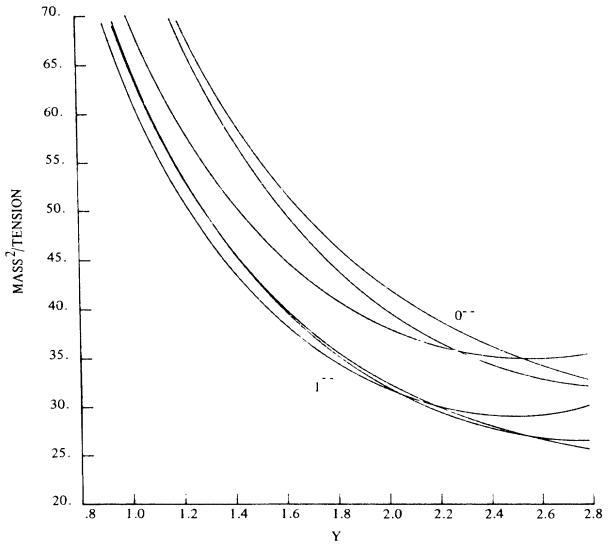

FIG. 9. R curves for the 0^{--} and 1^{--} states. In each curve we show the averages of the D-Padé fits to the t^5 and t^6 series as well as a diagonal 3-3 Padé which has a slightly different shape and tends to increase at high y. The general shape is quite similar to the scalar case leading to mass ratios which are not very different from the strong-coupling limit. The 2^{--} state is degenerate with the 1^{--} state in this order of the calculation.

two-scalar-glueball cut. One could therefore argue that both may be interpreted as pure cut effects, which this calculation cannot distinguish from resonances. However, judging from the known hadronic spectrum, we may expect to find many resonance states above the cut. In any case, it seems remarkable that we did not find a scaling result much lower than this cut.

All the negative charge-conjugation states which we have calculated need more than two gluonic fields for their description in the continuum field-theoretic formulation. This can be used as a reason for expecting them to lie higher than the scalar state which is bilinear in the gluonic fields.[10] Our results are in agreement with this argument although our calculation is based on a completely different formulation. So far we do not have any other source with which we can compare our results. An experimental verification of these glueball states is still lacking, and Monte Carlo calculations of lattice QCD have not yet produced a description of this part of the spectrum. Hopefully all will converge in the future to form a clear prediction and confirmation of the spectrum in the pure-glue sector.

ACKNOWLEDGMENTS

One of us (D.H.) would like to thank the theory groups of LBL and SLAC for their kind hospitality during the period when most of this work was done. One of us (C.P.D.) would like to thank the theory group of TRIUMF for its kind help. We are grateful to SLAC and TRIUMF for making it possible to complete the work reported here. This work was supported in part by the U.S.-Israel Binational Science Foundation.

[1]D. Horn and M. Weinstein, Phys. Rev. D **30**, 1256 (1984).
[2]D. Horn, M. Karliner, and M. Weinstein, Phys. Rev. D **31**, 2589 (1985).
[3]C. P. van den Doel and D. Horn, Phys. Rev. D **33**, 3011 (1986).
[4]J. Kogut and L. Susskind, Phys. Rev. D **11**, 395 (1975).
[5]C. P. van den Doel, D. Horn, and A. Klatchko, Phys. Lett. **172B**, 399 (1986).
[6]R. C. Johnson, Phys. Lett. **114B**, 147 (1982).
[7]J. Kogut, D. K. Sinclair, and L. Susskind, Nucl. Phys. **B114**, 199 (1976).
[8]J. E. Mandula, G. Zweig, and J. Govaerts, Nucl. Phys. **B228**, 109 (1983).
[9]Y. Dothan and D. Horn, Nucl. Phys. **B114**, 400 (1976).
[10]V. A. Novikov, M. A. Shifman, A. I. Vainshtein, and V. I. Zakharov, Nucl. Phys. **B191**, 301 (1981).